

We now calculate the damping of the spin waves. It is obvious that, at $T=0$, so long as the frequency satisfies the condition $-qv_F < \omega - IR < qv_F$, the waves are undamped. It can be seen from analysis of Eqs. (19) and (22) that the frequencies of the waves investigated satisfy this condition, and, therefore, the waves are undamped. At finite temperatures damping appears:

$$\text{Im } \omega = \frac{\pi}{4} \frac{\partial N}{\partial \mu} \frac{1}{N} \frac{\delta\mu + \omega}{qv_F} (\omega - IR) I n_0 \left\{ \frac{m(\omega - qv_F)^2}{2q^2} - \mu \right\}, \quad (26)$$

where $n_0(x)$ is the Fermi function. Using (19), we can convince ourselves that $\text{Im } \omega < 0$ for all the oscillations considered.

We shall now discuss why, despite the inverted spin populations, the spin waves are damped. The point is that the exchange interaction conserves the total spin. Therefore, it cannot itself lead to the creation of waves. The Landau damping is loss of kinetic energy of a wave to kinetic energy of random motion of the individual particles, with conservation of the moment. Thus, after the disappearance of a wave all that remains is the flipped spin of one electron. Of course, other interactions, e.g., interaction with a phonon via spin spin-orbit coupling, will lead to the creation of spin waves and to the

generation of these phonons. If further damping mechanisms were absent we would have a laser situation. However, the usual mechanisms of damping of phonons are much stronger than the amplification associated with the creation of spin waves, and, therefore, a state with nonequilibrium orientation of the spins is stable.

I wish to express my gratitude to M. I. D'yakonov, V. I. Perel', G. E. Pikus and E. F. Shender for interesting discussions.

¹A. G. Aronov and G. E. Pikus, *Fiz. Tekh. Poluprovodn.* **10**, 1177 (1976) [*Sov. Phys. Semicond.* **10**, 698 (1976)]; A. G. Aronov, *Pis'ma Zh. Eksp. Teor. Fiz.* **24**, 37 (1976) [*JETP Lett.* **24**, 32 (1976)]; *Zh. Eksp. Teor. Fiz.* **71**, 370 (1976) [*Sov. Phys. JETP* **44**, 193 (1976)].

²B. P. Zakharchenya, *Proc. Eleventh Intern. Conf. on Physics of Semiconductors, Warsaw, 1972*, publ. by PWN, Warsaw (1972), p. 1315; G. Lampel, *Proc. Twelfth Intern. Conf. on Physics of Semiconductors, Stuttgart, 1974*, publ. by Teubner, Stuttgart (1974), p. 743.

³R. M. White, *Quantum Theory of Magnetism*, McGraw-Hill, N. Y., 1970 (Russ. transl., Mir, M., 1972).

⁴S. Schultz and G. Dunifer, *Phys. Rev. Lett.* **18**, 283 (1967).

Translated by P. J. Shepherd

Bound states of fast electrons axially channeled in the single crystals

V. V. Kaplin and S. A. Vorob'ev

Nuclear Physics Institute of the Tomsk Polytechnic Institute
(Submitted December 7, 1976)
Zh. Eksp. Teor. Fiz. **73**, 583-586 (August 1977)

A model of bound states of channeled fast electrons in crystals is developed. The case of axial channeling of particles with $E = 0.5-15$ MeV along the principal crystallographic directions of silicon is considered in detail. The essential role of the high-lying states in anomalous passage through the crystals is demonstrated. A criterion is determined for separating deep-lying electronic states that determine the orientation dependence of the anomalous strong elastic scattering by atomic chains. It is shown that the deep-lying states are transformed into strongly absorbed states when the electron energy is increased. The quantitative data are used to discuss the angular distributions obtained by electron diffraction with an ESG-2.5 MeV accelerator. The bound-state model is used to explain the orientation dependences of the anomalous Rutherford scattering of electrons in single crystals. The orientational passage of relativistic electrons through thin crystals is also discussed. The energy dependence of the formation of bound states and the influence of neighboring atomic chains on the electron motion are considered. The possibility of realizing bound states of the molecular type in single crystals is discussed.

PACS numbers: 61.80.Mk

Under certain conditions of the passage of charged particles through single crystals, the correlation in the scattering of periodically disposed atoms becomes appreciable, thereby changing the character of the elastic and inelastic collision processes. New phenomena such as channeling and blocking of fast heavy positively charged particles and the ensuing secondary orientational effects have been investigated in sufficient detail and have found practical applications.^[1-3] To some de-

gree of approximation, the principal regularities and physical premises developed for the case of heavy charged particles can be extended to orientational effects that take place when fast electrons and positrons pass through single crystals.^[3,4] However, many features, such as the small particle mass, the effects of positron annihilation, or the negative sign of the electron charge, call for an independent study of the orientational phenomena involving electrons and positrons.

In^[5], on the basis of semiclassical diffraction theory, it was proposed to interpret the classical trajectories of the electrons channeled in single crystals as bound Bloch waves in wave theory. At the same time, in the calculation of the passage of electrons by dynamic diffraction theory, a noticeable concentration of the electron density on atomic chains was obtained and attributed to the establishment of bound states of particles with the atomic rows.^[6] These bound states of relativistic electrons were investigated earlier both experimentally, by a "transmission" method, and theoretically using the model of classical "rosetons."^[7,8] The purpose of the present paper is to develop a quantum-mechanical model of bound states of fast electrons in single crystals and to compare its main results with the parameters of the experimentally obtained angular distributions and orientation dependences. In our opinion, the treatment of bound states can extend the scope of the known dynamic model of diffraction of electron waves^[9] and contribute to the understanding of the relation between this theory and the theory of channeling of charged particles. Within the framework of the developed model, we succeed in explaining in a unified manner two observed phenomena, absorption and anomalous passage of electrons through single crystals, and obtain the orientation dependences and the angular distributions of the scattered particles. We present here the results of a discussion of the anomalous deep penetration of relativistic electrons in crystals with the inelastic processes neglected.

1. STRONGLY BOUND STATES OF FAST ELECTRONS WITH ONE CHAIN OF ATOMS

If the spin is disregarded in the potential $U(x, y, z)$ of the crystal lattice, a relativistic electron should be described by a wave function $\Phi(x, y, z)$ which is a solution of the Klein-Gordon equation

$$(\hbar^2 c^2 \nabla_{xy}^2 + [E - U(x, y, z)]^2 - m_0^2 c^4) \Phi(x, y, z) = 0, \quad (1)$$

where $m_0 = \gamma' m$, $\gamma' = (1 - v^2/c^2)^{1/2}$ is the relativistic factor. The three-dimensional potential $U(x, y, z)$ of the interaction of the electron with the single crystal can, however, be represented as a superposition of continuous potentials $U(r)$ of the atomic chains.^[10]

$$U(x, y, z) \sim U(x, y) = \sum_r U(r).$$

The two-dimensional treatment of the passage of charged particles through single crystals is dictated by the fact that the fast electrons are controlled predominantly by the average potential along the direction of its motion (the z axis). This follows both from the classical and from the quantum-mechanical analysis.^[2,11] The problem of the passage of electrons through a crystal lattice is made much simpler by the continuity of the cylindrical-symmetry potential $U(r)$ in the z direction. If the xy plane is perpendicular to the axis of the atomic row we obtain the equation

$$-(\hbar^2/2m) \nabla_{xy}^2 \Phi(x, y) + U(x, y) \Phi(x, y) = E_{\perp} \Phi(x, y) \quad (2)$$

by writing $\Phi(x, y, z) = \Phi(x, y)\Phi(z)$ and separating the variables in (1). This equation is the nonrelativistic Schrödinger

equation for a negatively charged particle with a relativistic mass m . The function $\Phi(z)$ is the solution of the Klein-Gordon equation for a free particle, i. e., a relativistic plane wave. If the average potential of the atomic row is "cut off" at a distance r_0 (the "muffin-tin potential" approximation for the xy plane), $U(x, y) = U(r)$ at $r \leq r_0$ and $U(r) = \text{const}$ $r > r_0$, then the so called associated wave function $\Phi_{\mathbf{k}}(r)$,^[12] used to construct the wave function

$$\Phi_{n\mathbf{l}}(r) = \sum_{\mathbf{q}_{\perp}} a_{\mathbf{k}-\mathbf{q}_{\perp}} \Phi_{\mathbf{k}-\mathbf{q}_{\perp}}(r)$$

(\mathbf{q}_{\perp} is the vector of the reciprocal two-dimensional lattice of the scattering potentials and $a_{\mathbf{k}-\mathbf{q}_{\perp}}$ are coefficients to be determined), takes the form

$$\Phi_{\mathbf{k}}(r) = \begin{cases} \exp\{i\mathbf{k}_{\perp} \mathbf{r}\}, & r > r_0 \\ \sum_{\mathbf{l}} C_{\mathbf{l}} R_{n\mathbf{l}}(r) \exp\{i\mathbf{l}\varphi\}, & r \leq r_0 \end{cases} \quad (3)$$

Here $C_{\mathbf{l}}$ is determined from the condition that the parts of the solution be matched together at $r = r_0$; $R_{n\mathbf{l}}(r)$ is the radial part of the wave function of the electron in the field of the atomic chain, and is determined from the equation

$$\frac{\hbar^2}{2m} \left[\frac{d^2 R_{n\mathbf{l}}(r)}{dr^2} + \frac{1}{r} \frac{dR_{n\mathbf{l}}(r)}{dr} - \frac{l^2}{r^2} R_{n\mathbf{l}}(r) \right] = [U(r) - E] R_{n\mathbf{l}}(r). \quad (4)$$

In quantum theory of solids^[12] it is shown that within the framework of the model assumed by us for the analysis of the motion of strongly bound electrons ($E_{\perp} < U(r = r_0)$) it suffices to consider the solutions of Eq. (4). The continuous potential $U(r)$ of the atomic chain can be approximated by a potential function^[13]

$$U(r) = -cZe^2 a_{TF}/rd, \quad (5)$$

where Z is the atomic number of the potential, a_{TF} is the Thomas-Fermi screening radius, d is the interatomic distance in the row, and c is a constant equal, for example, to 1.4 for the $\langle 111 \rangle$ atomic rows of silicon. The solutions of (4), as is well known, are wave functions of the type

$$R_{n\mathbf{l}}(r) = \frac{1}{\sqrt{r}} e^{-\pi r/a} \left(\frac{r}{a} \right)^{|l|+1/2} \sum_{k=0}^n a_k \left(\frac{r}{a} \right)^k, \quad (6)$$

where n and $|l|$ are equal to 0, 1, 2, ...; $a = \hbar^2 d/cmZe^2 a_{TF}$ is a characteristic length that depends on the particle energy; the coefficients a_k are given by the relation

$$a_{k+1} = 2a_k \left[\gamma(k+|l|+1/2) - 1 \right] / (k+1)(k+1+2|l|), \\ \gamma = (n+|l|+1/2)^{-1}.$$

The coefficient a_0 is determined from the condition of the normalization of the wave function

$$2\pi \int_0^{\infty} |R_{n\mathbf{l}}(r)|^2 r dr = 1.$$

The eigenvalues of the transverse energy are given in the two-dimensional problem by the expression

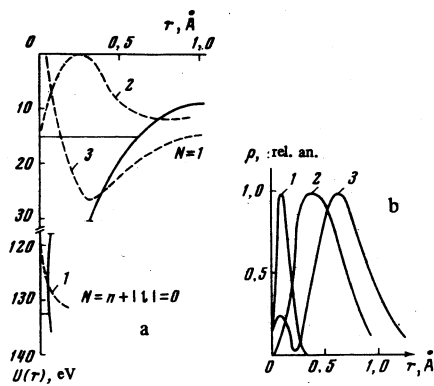


FIG. 1. a) The continuous potential $U(r)$ of the interaction of a fast electron with the atomic row $\langle 111 \rangle$ Si (thick curve), the self-energy levels and the wave functions of the strongly bound state $1s$, $2p$, and $2s$ (curves 1, 2, and 3, respectively) at an electron energy $E = 1.0$ MeV. b) Distribution densities of electrons in the $1s$, $2p$, and $2s$ states (curves 1, 2, 3, respectively).

$$E_{LN} = -\frac{c^2 m Z^2 e^4 a_{TF}^2}{2 \hbar^2 d^2 (n + |l| + 1/2)^2}, \quad N = n + |l|. \quad (7)$$

The limiting energy E_{1im} , at which the level of the N -th state lies below the crest of the potential barrier separating the atomic chains, can be obtained in the form

$$E_{1im} = E_0 (m_{1im} / m_0 - 1), \quad (8)$$

where

$$m_{1im} = \frac{2 \hbar^2 d U(d/2) (N + 1/2)^2}{c^2 Z^2 e^4 a_{TF}^2} \quad (9)$$

is determined from the condition $E_{LN} = U(r_0)$, $r_0 = d_r/2$ is half the distance between the atomic rows, and E_0 and m_0 are respectively the energy and rest mass of the electron. The energy E_{1im} of the first state ($N=0$) is substantially lower, in contrast to the second state, the level of which appears in the potential well of $\langle 111 \rangle$ Si at a limiting energy $E_{1im} = 0.75$ MeV. We have previously^[14] determined the limiting energy at which bound trajectories exist, using the concept of the critical approach of the channeled particle to the atomic row, and obtained $E_{1im} = 0.20$ keV for $\langle 100 \rangle$ NaCl, which is much lower than the value of E_{1im} determined by quantum conditions.

Figure 1 shows the levels of the transverse energy of the bound states of the electrons, the wave functions and the distribution densities of the electrons at energy $E = 1.0$ MeV for the states $N=0$ and 1 (curves 1 and 2 for states $l=0$ and curve 3 for $l=\pm 1$). When moving in a single-crystal lattice in a state $N=0$ ($1s$ state in the terminology of^[15,16]), the electron is located mainly at a distance $r \approx 0.05$ Å from the atomic row—in the region of the maximal nuclear and electron densities. In the classical treatment, the analogs of the motion of an electron in a crystal with formation of a $1s$ state are quasi-sinusoidal trajectories with small amplitude of the oscillation about the row. An electron in the excited states $2s$ and $2p$ will be located mainly at distances $r \approx 0.4-0.6$ Å (Fig. 1b). Such a passage of the particles

through the lattice corresponds in a classical model to motion along long-range quasi-sinusoidal and roseton trajectories.^[15,16] The type of the realized bound state will be the decisive factor in the character of the interaction of the fast electrons with atomic lattice. For example, if the probability of the passage of electrons near atomic nuclei is larger in the realization of the state than in random motion, i. e., if the condition

$$K = \frac{2S}{a_T^2} \int_0^{a_T} |\Phi_{nl}(r)|^2 r dr > 1 \quad (10)$$

is satisfied (where a_T is the average distance of the thermal displacements of the atoms from the axis of the atomic row and S is the cross section area of the crystal per chain), then the yield of the processes that require small impact parameters increases and the state becomes strongly interacting. In the concrete case of $\langle 111 \rangle$ Si and at an electron energy $E = 1.0$ MeV we have $K > 1$ for the $1s$ and $2s$ states. As will be shown below, these states explain for the most part the increases of the Rutherford scattering,^[17] of the characteristic x radiation,^[18] as well as of the back-scattering coefficient,^[19] observed in experiment when parallel beams of electrons are incident along single-crystal axes. For the $2p$ state in the field of the atomic row $\langle 111 \rangle$ Si at an electron energy $E = 1.0$ MeV we have $K < 1$ and the states interact weakly with the nuclei of the single-crystal atoms. It is probable that the anomalous passage of electrons measured in^[7,8,13,20] is in fact the consequence of the realization of such excited states. In each concrete case, for definite single crystals, crystallographic directions, and electron energies, using the criterion (10), we can distinguish between strongly and weakly interacting realized states. With increasing electron energy, the number of levels of the bound motion increases as a result of the increase of m and is determined by the equality

$$N' = N_{max} + 1 = [-A^2/U(d/2)]^{1/2} + 0.5, \quad (11)$$

where

$$A = -\frac{cZe^2 a_{TF}}{\hbar d} \sqrt{\frac{m}{2}}$$

N_{max} is the quantum number of the higher bound states. Table I lists the positions of the levels for the electrons with energies $E = 0.5-10$ MeV in $\langle 111 \rangle$ Si. In particular, it is seen that when the electron energy is increased to $E = 10$ MeV the level $N=1$ (the $2s$ and $2p$ states) drops almost to the position of the level of the $1s$ state, which is characteristic of $E = 1.0$ MeV when $K > 1$. Thus, the $2p$ state is no longer strongly penetrating and is trans-

TABLE I.

E, MeV	N'	Positions of the levels E_{LN} , eV				
		1s	2s, 2p	3s-3d	4s-4f	5s-5g
1.0	2	434	45	—	—	—
2.0	2	422	25	—	—	—
6.0	4	570	65	36	48	—
10.0	5	1030	105	58	29	17.5

formed into a state that interacts strongly with the crystal atoms. It can be noted that the larger the number N of the state, the weaker its interaction with the nuclei or with the atomic electrons of the single crystal.

In Coulomb fields of atomic chains, other negatively charged particles can also be in bound states, for example π^- or μ mesons. Formulas (7) and (6) for the transverse self energies and wave functions of the mesic bound states are fully applicable to these mesons. The mass of the π^- meson is $273m_0$, and approximately 16 levels of bound states will be realized in the crystal at nonrelativistic velocities of these particles. As a result of the larger mass, the energy positions of the meson bound states will not have a clearly pronounced energy dependence. For concrete calculations, the wave functions in the form (6) are hardly suitable for mesons or high-energy electrons. We therefore propose to use wave functions of the Slater type, which in contrast to the hydrogen-like wave functions have simpler radial parts $F_N(r) = r^N e^{-\xi r}$, where ξ is a constant separately chosen for each state. This approximation does not introduce a substantial error in comparison with the error due to the choice of the model average potential of the row and subsequent construction of the wave function for the system of rows in the form of a linear combination of basis functions.

2. ANGULAR CHARACTERISTICS OF STRONGLY BOUND STATES

We consider in greater detail the passage of a $2p$ -state electron with energy $E = 1.0$ MeV along $\langle 111 \rangle$ Si, since this state is the most strongly penetrating. The average distance at which the particle passes near the atomic row is in this case

$$\langle r \rangle = 2\pi \int_0^\infty R_{01}(r) r R_{01}(r) dr = 3a, \quad (12)$$

The average transverse kinetic energy is correspondingly

$$\langle E_\perp \rangle = -\frac{\hbar^2}{m} \iint R_{01}(r) e^{-i\varphi} (\nabla_{r,\varphi}^2 R_{01}(r) e^{i\varphi}) r dr d\varphi. \quad (13)$$

The energy $\langle E_\perp \rangle$ determines the average emergence angle of the electron from single crystal

$$\langle \theta \rangle = (\langle E_\perp \rangle / E)^{1/2} = \hbar\gamma / a(2mE)^{1/2}. \quad (14)$$

Table II lists the calculated values of $\langle \theta \rangle$ for different electron energies in comparison with the experimentally obtained radii of the rings in the angular distributions for the direction $\langle 111 \rangle$ Si. The reason why the calculated

TABLE II.

E , MeV	$\langle r \rangle$, Å	$\langle E_\perp \rangle$, eV	$\langle \theta \rangle$, deg	θ_{\max} , deg	R , deg
0.8	0.295	12.7	0.285	0.17	0.18
1.0	0.254	15.0	0.27	0.15	0.15
1.2	0.230	16.3	0.255	0.14	0.13
1.5	0.202	19.7	0.25	0.135	0.10
2.0	0.154	25.1	0.245	0.13	-

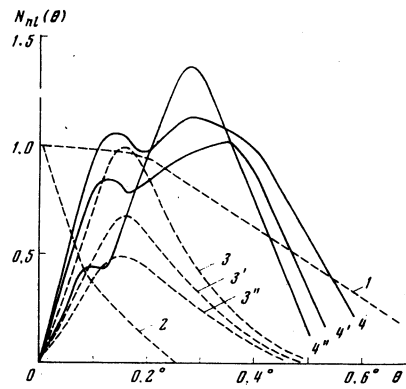


FIG. 2. Calculated angular distributions of the electrons passing along $\langle 111 \rangle$ Si in the $1s$ and $2s$ states (curves 1 and 2 respectively) and in the $2p$ states at electron energies $E = 1.0$, 1.2 , and 1.5 MeV (curves 3, 3', and 3'', respectively). Curves 4, 4', and 4'' are results of photometry of the electron diffraction patterns of the electron beams with energies $E = 1.0$, 1.2 , and 1.5 MeV (similar to Fig. 5a below).

value of $\langle \theta \rangle$ does not agree well with the ring radius R is assumed by us to be the fact that the function

$$P(\theta) = 2\pi k \theta |\Phi(k_\perp)|^2 dk_\perp / d\theta \quad (15)$$

(where $k = [(m + m_0)E]^{1/2} / \hbar$ and $k_\perp \sim k\theta$ are respectively the values of the total and transverse wave vectors of the electron), which describes the θ -distribution of the electrons passing through the single crystal in a state with wave function $\Phi(k_\perp)$ in the momentum representation, decreases slowly in the region of large angles. Therefore the average emergence angle $\langle \theta \rangle$ will lie on the maximum of the distribution (15).

Using a representation of the wave function in the form

$$\Phi(k_\perp) = 2 \int_0^\infty \int_0^{2\pi} \exp(-ik_\perp r \cos \varphi) R_{nl}(r) e^{i\varphi} r dr d\varphi \quad (16)$$

and subsequently expanding the exponential function in Bessel functions, we obtain from (15) for the $2p$ state the angular dependence of the intensity on a screen placed behind the crystal:

$$P'(\theta) = 243a^2 k^3 \theta^2 / (1 + \theta^2 / a^2 k^2 \theta^2)^5. \quad (17)$$

This dependence for electrons with energy $E = 1.0$ MeV is shown in Fig. 2 (curves 3) in comparison with the results of photometry (curves 4) of the electron diffraction pattern behind a crystal $\langle 111 \rangle$ Si of $5 \mu\text{m}$ thickness. Satisfactory agreement is obtained between the radius R of the ring on the electron diffraction pattern and the position of the maximum θ_{\max} of the calculated curves.

Figure 2 shows also the calculated angular distributions for the $1s$ and $2s$ states (curves 1 and 2 respectively). In contrast to the $2p$ state, the maximum of the intensity is expected in this case to be in the direction of the crystallographic axis. However, as shown by comparison with experiment, no such states are observed in our case. It is probable that owing to the strong inter-

action with the atoms the electrons manage in this case to go over to higher levels during the time of passage through the crystal. These high-lying states, which are not connected with individual rows, result in an enhancement of the intensity on the electron diffraction pattern in the form of six spots, which cannot be explained within the framework of the model of strongly coupled states with individual atomic chains. Thus, it is precisely the $2p$ state which is responsible for the internal ring. The good agreement with the experimental data of the calculated angular distributions of the electrons with energies 1.0 and 2.0 MeV was noted also behind the crystal $\langle 111 \rangle$ W.^[21,22]

Comparison in our case of the values of R and θ_{\max} at energies $E=1.0, 1.2,$ and 1.5 MeV (see Fig. 2 and Table II) shows that a better agreement between them is observed at lower electron energies. In a real case, the lattice atoms execute thermal vibrations and the potential $U(r)$ of the atomic row has a finite depth, on account of the "smearing" of the effective charge of the chain. With increasing energy of the fast electrons, the energy level of the state will not drop as rapidly as for an infinitely deep well. Since the angular width of the particle distribution behind the single crystal is proportional to $\langle \theta \rangle$ [Eq. (14)], the experimental radii (curves 4, 4', and 4'') of the angular intensity distributions decrease more strongly in comparison with calculation (curves 3, 3', and 3''), respectively.

The dependence of the formation of bound states on the transverse energy can be traced by representing the plane wave incident on the single crystal at $z=0$ in the form

$$\exp(ik_{\perp}r) = \sum_{n_i} a_{n_i} R_{n_i}(r) \exp(il\varphi).$$

The coefficients a_{n_i} are therefore

$$a_{n_i} = \int_0^{\infty} \exp(ik_{\perp}r) R_{n_i}^*(r) dr. \quad (19)$$

Now the quantity $|a_{n_i}|^2$ will determine the probability density for the production of states with wave function $R_{n_i}(r)$. This probability depends on the angle of incidence φ of the external wave on the single crystal, and is given for the $2p$ state at $k_{\perp} \sim k\varphi$ by an expression of the form^[13,21]

$$N(\varphi) = |a_{n_i}|^2 = \frac{124\hbar^2 d^2 k^2 \varphi^2}{m^2 Z^2 e^4 a_{TF}^2 (1 + 9/4 a^2 k^2 \varphi^2)^5}. \quad (20)$$

It must be noted that (20) is similar in form to the dependences obtained by us earlier, in the classical model, for the fraction of the captured electrons of a parallel beam by "roseton" trajectories near the atomic row.^[13,14] With increasing angle φ , expression (20) shows a decrease of the probability of realization of the bound $2p$ state. Accordingly, in our experiment, we observed a decrease of the intensity of the ring when the crystal was inclined in the angle region close to the calculated one.^[23] The evolution of $N(\varphi)$ with changing energy shows that when the electron energy is increased the capture of particles into a bound $2p$ state decreases substantially, and

this possibly explains the absence of rings on the electron diffraction patterns at $E=2.0$ and 2.5 MeV.^[13,23] Furthermore, the self-energy level of the state drops deeper into the potential well, and the maximum of the distribution of the electron density approaches the atom row, therefore the stability and the lifetime of the state decrease. The energy E_T of the transformation of the $2p$ state from a deeply penetrating state into one that interacts strongly with the lattice can be estimated from the condition $K=1$, using a relation simpler than (10), namely

$$K = SP(r)/2\pi r \quad (21)$$

for r in range $0 < r < a_T$. At $S \approx \pi r_0^2$ we have for $\langle 111 \rangle$ Si, i. e., $r_0 = 5a_{TF}$ and $r \approx a_T \approx 0.5a_{TF}$

$$45a_{TF}^4 \exp(-2a_{TF}/3a) = 8a^3. \quad (22)$$

Expanding the exponential in a series and taking into account the first four terms, we obtain $m = \hbar^2 d / 2.28 Ze^2 a_{TF}$, which corresponds to a transformation energy $E_T = 2.2$ MeV.

For bound states of the type $1s$ and $2s$, calculation shows that the probability of their realization has a maximum when the external plane wave is incident strictly in the direction of the atomic chain. The dependences of the formation of these states on the angle of incidence of the electrons in the single crystal, obtained for $\langle 111 \rangle$ Si at an electron energy $E=1.0$ MeV are similar to curves 1 and 2 on Fig. 2.

We have also calculated the dependences of probabilities of formation of $1s$ and $2s$ states as strongly inter-

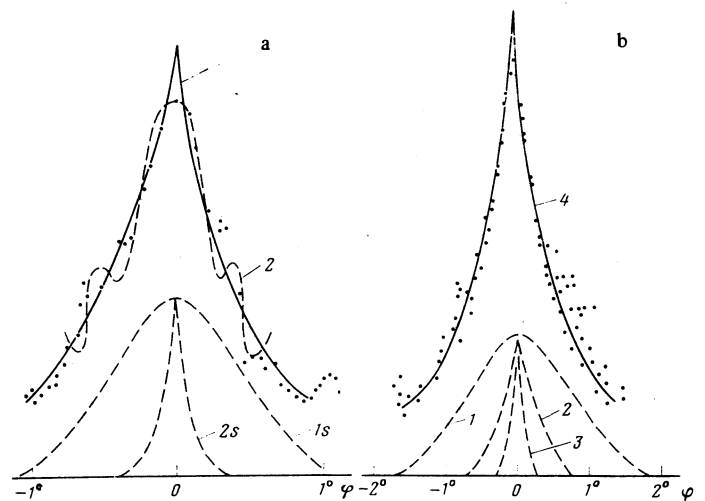


FIG. 3. a) Calculated summary orientation dependence of the realization of the $1s$ and $2s$ states for $\langle 100 \rangle$ Si and electrons with $E=1.5$ MeV—curve 1. In the lower part are shown the contributions of the individual states. Curve 2—91-beam calculation by the dynamic theory of the diffraction of electron waves.^[17] Points—result of measurements of the Rutherford scattering.^[17] b) Orientation dependences of the realization of $1s$, $2s$, and $3s$ states for $\langle 110 \rangle$ Si and electrons with energy $E=1.5$ MeV—curves 1, 2, and 3, respectively; curve 4—results of their summation. Points—results of measurement of the Rutherford scattering.^[17]

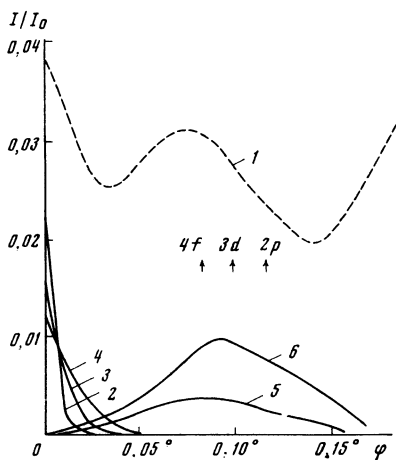


FIG. 4. Orientation dependence of the passage of the electrons with $E = 15$ MeV through $\langle 111 \rangle$ Si of thickness $1.4 \mu\text{m}$ —curve 1^[24] and the calculated orientation dependences of the realization of the $6s$, $5s$, $4s$, $6h$, and $5g$ states—curves 2, 3, 4, 5, and 6, respectively.

acting with the atomic lattice for the $\langle 100 \rangle$ Si axis and an energy $E = 1.5$ MeV. Figure 3a shows a comparison of the summary angular dependence of the realization of the $1s$ and $2s$ states (curve 1) and the experimentally obtained dependence of the yield of the Rutherford scattering of electrons on the angle of inclination of the single crystal.^[17] The figure shows also the results of a 91-beam calculation by the dynamic theory of the diffraction of electron waves, carried out in^[17] (Fig. 2). It is seen that calculation by the theory of strongly-coupled states of the channeled electrons agrees well with experiment.

A recent experimental investigation of the passage of electrons with $E = 15$ MeV through $\langle 111 \rangle$ Si of thickness $t = 1.4 \mu\text{m}$ ^[24] has revealed at the center of the orientation dependence (Fig. 4, curve 1) a narrow maximum, which in our model can be due to the high-lying state of the s type. Figure 4 shows the calculated orientation dependences of the excitation of high-lying $6s$, $5s$, $4s$, $6h$, and $5g$ states. Comparison with the experimental dependence shows that the central maximum of the anomalous passage can be formed by the state with $l = 0$ and the lateral maximum can be due to states $l \neq 0$. The states with $N = n + |l| < 4$ are strongly interacting in accordance with (10) and are not observed in the experiment. The maxima of the $4f$, $3d$, and $2p$ states are shifted sideways from the observed lateral peak. The reasonable agreement between the results favors the developed model for the passage of fast electrons through an atomic lattice, which, when sufficiently developed, will probably be able to extend the scope of the known dynamic theory and contribute to the understanding of its relation with the theory of channeling of charged particles.

3. INFLUENCE OF NEIGHBORING ATOMIC ROWS. BOUND STATES OF MOLECULAR TYPE

The angular distributions of the electron behind crystals depend substantially on the considered crystallographic direction. For example, the experimental pictures obtained by us for the directions $\langle 100 \rangle$ and $\langle 110 \rangle$

of Si, in contrast to the $\langle 111 \rangle$ direction, have no noticeable ring in the central part of the electron diffraction pattern, Fig. 5.^[23] As shown by an analysis of the ratio of the energies of the electrons and potentials of the corresponding atomic rows, no pronounced bound state is produced in the case of the $\langle 100 \rangle$ axis. The level of the $2p$ state lies above the position of the potential barrier, and the electrons are not strongly coupled. These electrons, however, are not free, since their transverse momentum varies with time. Whereas in the case of the $\langle 111 \rangle$ axis the bound-state electrons can transfer from one free atomic row to another only via tunneling through the potential barrier of the separating chain, in the case of the $\langle 100 \rangle$ direction they migrate in the xy plane along the lattice, in analogy with the valence electron in the single crystal, being located at large distances from the axes of the atomic rows and therefore having a large penetrating ability. This leads to the formation of electron states that are bound to the atomic planes. Such states are made up of wave functions (6) with alternating signs of the quantum number l . In the classical treatment they are viavons with small periods of oscillation of the trajectory in the xy plane. The ratio of the motion of the fast electrons along such trajectories ("crimped motion") and the pure planar effects of electron channeling were discussed by us in detail in^[25]. Owing to the important role of the plane-wave part in the wave function of the weakly-coupled $2p$ state (3), the electron density will be maximal in the gaps between the atomic rows, and the quasi-free state for the $\langle 100 \rangle$ axis will give rise to four spots of increased intensity in the central part of the electron diffraction pattern (Fig. 5).

If the energy of the electrons is increased, then the level drops and a strongly bound state is produced, characterized by an azimuthal homogeneity of the annular distribution. However, according to expression (20) the probability of its capture into this state decreases and we may encounter again the situation considered for channeling of electrons with energy $E \geq 2.0$ MeV along the $\langle 111 \rangle$ axis, where the theoretically expected ring was not observed in the experiment.

To consider the weakly bound states we must solve the wave equation for the periodic potential of the xy plane. The solution of this equation is given according to the Bloch theorem by

$$\Phi_{\mathbf{k}_\perp}(\mathbf{r}) = \sum_{\mathbf{q}_\perp} a_{\mathbf{k}_\perp - \mathbf{q}_\perp} \Phi_{\mathbf{k}_\perp - \mathbf{q}_\perp}(\mathbf{r}), \quad (23)$$

where \mathbf{q}_\perp is the reciprocal two-dimensional lattice vec-

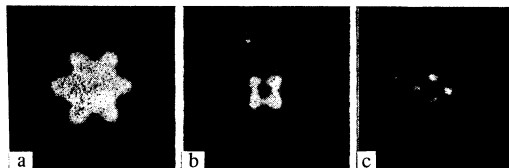


FIG. 5. Electron-diffraction patterns of silicon crystals of thickness $t \approx 5 \mu\text{m}$ for electrons with $E = 1.0$ MeV^[23] at orientations: a) $\langle 111 \rangle$ Si; b) $\langle 100 \rangle$ Si; c) $\langle 110 \rangle$ Si.

tor and the coefficient $a_{k_{\perp}-q_{\perp}}$ is to be determined. Using (23) as a trial function for the determination of the self-energy ε by a variational method, we find that the expansion coefficient should satisfy equations of the type^[12]

$$\{(k_{\perp}-q_{\perp})^2+\varepsilon\}a_{k_{\perp}-q_{\perp}}+\sum_{q_{\perp}'}\Gamma_{q_{\perp}q_{\perp}'}a_{k_{\perp}-q_{\perp}'}=0, \quad (24)$$

where $\Gamma_{q_{\perp}q_{\perp}'}$ is an integral containing the functions $\Phi_{k_{\perp}-q_{\perp}}$, $\Phi_{k_{\perp}-q_{\perp}'}$ and a Hamiltonian with a periodic potential. The calculation reduces now to the complicated procedure of solving the system of nonlinear equations (24). We note that Eq. (24) coincides exactly with the equations of the dynamic theory of the diffraction of electron waves in a crystal^[9] if $\Gamma_{q_{\perp}q_{\perp}'}$ is treated as the Fourier components of $V_{q_{\perp}q_{\perp}'}$, the effective potential.

We call attention to an interesting singularity in the arrangement of the atomic rows in the case of the crystallographic direction $\langle 110 \rangle$ Si. In contrast to the axes $\langle 111 \rangle$ and $\langle 110 \rangle$, the atomic chains are disposed here in pairs and there is a preferred direction of the overlap of the wave function of the states connected with the individual rows. It is therefore necessary to consider bound states not of the atomic type but, breaking up the xy plane into elementary areas S belonging to a pair of rows, to operate with bound states of the molecular type. Disregarding the interaction of the channeling electron with the other atomic chains and representing the potential of the pair as a superposition of single-chain potential functions, we can calculate the molecular orbitals for a weak overlap of the potentials of the chains by writing down for the resultant wave function

$$\Phi(\mathbf{R})=\alpha\Phi_{n_1}(\mathbf{r}_1)+\beta\Phi_{n_2}(\mathbf{r}_2), \quad (25)$$

where $\alpha=\beta$ and $\alpha=-\beta$ respectively for the symmetrical and antisymmetrical states. At small values of E_{LN} the overlap of $\Phi_{n_1}(\mathbf{r})$ is small and the states that interact strongly with the lattice atoms can be calculated by using the single-chain approximation. Figure 3b shows a comparison of the experimentally obtained^[17] orientation dependence of the Rutherford scattering of the electrons with energy $E=1.5$ MeV for $\langle 110 \rangle$ Si and the calculated summary angular dependence of the realization of the 1s, 2s, and 3s states (curves 1, 2, and 3) with the contributions determined by the ratio

$$n_{00}:n_{10}:n_{20}=(N_{00}|\Phi_{00}|^2):(N_{10}|\Phi_{10}|^2):(N_{20}|\Phi_{20}|^2)=1:1:1.$$

In the analysis of the angular distributions of the fast electrons produced in the case of $\langle 110 \rangle$ Si by realization of high-lying states, the overlap is large and the approximation (25) for the wave function is incorrect. It is probably reasonable to approximate the potential of a pair of chains by a two-dimensional potential box of finite depth and regard the smeared states as quasimolecular.

4. CONCLUSION

The foregoing discussion shows that the concept of bound states of fast electrons in the course of channeling offers great possibilities for the explanation of the singularities of the passage through single crystals. With-

in the framework of the developed model we can use besides the concepts of wave mechanics, the easily visualized representations of classical trajectories for both strongly coupled and weakly coupled electrons in a lattice. In our opinion, particular interest attaches to the "transition channeling" of almost-free electrons, which is due to the formation of quasibound states with chains of atomic rows in the representation of the superposition of wave functions of high-lying states. The regime of "transition channeling" due to above-the-barrier states, will be responsible for the strong passage of electrons in the crystal, since the maximum of the electron distribution density occurs in this case in region far from the axes of the atomic rows. Our experimental investigations have shown that when the crystal thickness is decreased the first to vanish is the internal ring, and the symmetrical spots of the intensity still remain on the electron diffraction pattern.^[13,20] This agrees with the present model, in which the ring of increased intensity is attributed to strongly coupled channeling, and the symmetrical spots are attributed to above-the-barrier states. When moving in strongly bound states, the fast electrons will be closer to the axis of the atomic row than electrons in the above-barrier states, as a result of which they become "dechanneled" by going over primarily to high-lying levels. It is appropriate to note that above-barrier states play a special role also in channeling of positively charged particles.^[26] In the latter case, however, they are responsible for the enhancement of the yield of processes that require small impact parameters of the interaction, owing to the increase in the particle density in the positions of the atomic rows.

The model developed for the channeling of electrons has enabled us to predict the possibility of observing electromagnetic radiation generated in spontaneous radiative transitions between energy levels of bound states.^[27] In the classical analysis, the trajectories of the bound motion of the electrons with the atomic rows or planes in crystals, this electromagnetic radiation is the analog of the known synchrotron or undulatory radiation in external macrofields. The proposed theoretical approach has attracted definite interest, and estimates of the characteristics of the radiation of relativistic positrons in planar channeling were recently obtained in similar fashion.^[28] In the electron energy region considered by us, the frequency of the radiation occupies principally the visible region of the spectrum, but increases with increasing inclination of the crystal, and at definite inclination angles we obtain a source of ultraviolet radiation. The angular distribution of the radiation of the channeled electrons is confined to the interior of the Cerenkov-radiation zone, and the form of its orientation dependence should duplicate the calculated angular dependences of the probability of capture into high-lying bound states. By choosing a definite configuration of external electromagnetic fields we can hope to obtain a source of stimulated monochromatic radiation, which is adjustable in a wide range of frequencies up to the x-ray region. When fast electrons move in bound states in a single crystal, one should expect coherent radiation of the excited atoms, of the type of

the structural Cerenkov radiation considered earlier for the case of channeling of positively charged particles.^{12a)} The presented model of channeling of fast electrons suggests the possibility of polarization of the electron spins when the electron is scattered by a crystal, with formation of a bound state. In other words, if a bound state with an atomic chain is produced when a negatively charged particle, say an electron or a meson, with arbitrary spin orientation is incident on the crystal, then a fixed direction of the average spin of the particle takes place in one of the two directions that are allowed for this state. Thus, in the simple case when the $1s$ state is produced, we can obtain past the crystal particles with an average spin directed parallel or antiparallel to the direction of their motion. By varying the particle energy, the type of the crystal, and its inclination relative to the beam, it is possible, besides changing the form of the realized state, also to change the polarization of the spin of the electrons passing through the crystal. We can thus produce a source of polarized electrons or mesons, for use, for example, in accelerator technology and in experimental nuclear physics.

The authors are most grateful to A. F. Tulinov for constant interest in the work.

¹A. F. Tulinov, Usp. Fiz. Nauk 87, 585 (1965) [Sov. Phys. Usp. 8, 864 (1966)].

²J. Lindhard, K. Dan. Vidensk. Selsk. Mat.-Fys. Medd. 34, No. 14 (1965).

³D. S. Gemmell, Rev. Mod. Phys. 46, 129 (1974).

⁴S. A. Vorob'ev, Proc. 6th All-Union Conf. on the Physics of Interaction of Charged Particles with Single Crystals, Moscow State Univ. 1975, p. 191.

⁵M. V. Berry, B. F. Buxton, and A. M. Ozorio de Almeida, Radiat. Eff. 20, 1 (1973).

⁶K. Kambe, G. Lehmpfuhl, and F. Fujimoto, Z. Naturforsch. Teil A, 29, 1034 (1974).

⁷F. Fujimoto, K. Komaki, H. Fujita, N. Sumita, Y. Uchida, K. Kambe, and G. Lehmpfuhl, Atomic Collision Phenomena in Solids 2, Plenum Publ. Corp., New York, London, 1975, p. 547.

⁸A. Ya. Babudaev, V. V. Kaplin, and S. A. Vorob'ev, Phys. Lett. 45A, 71 (1973).

⁹P. B. Hirsch *et al.*, Electron Microscopy of Thin Crystals, Plenum, 1965.

¹⁰H. C. N. Nip and J. C. Kelly, Phys. Rev. 5B, 813 (1972).

¹¹M. V. Berry, J. Phys. C 4, 697 (1971).

¹²J. M. Ziman, Principles of the Theory of Solids, Cambridge Univ. Pr., 1965.

¹³V. V. Kaplin, S. V. Plotnikov, I. A. Tsekhanovsky, and S. A. Vorob'ev, Phys. Lett. 54A, 447 (1975).

¹⁴A. A. Vorob'ev, V. V. Kaplin, and S. A. Vorob'ev, Izv. Vyssh. Uchebn. Zaved. Fiz. No. 8, 79 (1975).

¹⁵H. J. Kreiner, F. Bell, R. Sizmann, D. Harder, and W. Hüftl, Phys. Lett. 33A, 135 (1970).

¹⁶H. C. H. Nip, M. J. Hollis, and J. C. Kelly, Phys. Lett. 28A, 324 (1968).

¹⁷E. Uggerhoj and F. Frandsen, Phys. Rev. 2B, 582 (1970); S. K. Andersen, F. Bell, F. Frandsen, and E. Uggerhoj, Phys. Rev. 8B, 49 13 (1973).

¹⁸B. D. Grachev, A. P. Komar, Yu. S. Korobochko, and V. I. Mineev, Pis'ma Zh. Eksp. Teor. Fiz. 4, 24 (1966) [JETP Lett. 4, 163 (1966)]; A. P. Komar, B. D. Grachev, Yu. S. Korobochko, and V. I. Mineev, Fiz. Tverd. Tela (Leningrad) 10, 1547 (1968) [Sov. Phys. Solid State 10, 1222 (1968)].

¹⁹A. A. Vorob'ev, A. N. Didenko, I. A. Tsekhanovsky, and S. A. Vorob'ev, Phys. Status Solidi 6A, 389 (1971); A. A. Vorob'ev, A. Ya. Babudaev, S. A. Vorob'ev, and V. V. Kaplin, Fiz. Tverd. Tela (Leningrad) 14, 3310 (1972) [Sov. Phys. Solid State 14, 2808 (1973)].

²⁰S. A. Vorob'ev, S. V. Plotnikov, and I. A. Tsekhanovskii, Pis'ma Zh. Tekh. Fiz. 1, 968 (1975) [Sov. Tech. Phys. Lett. 1, 418 (1975)].

²¹K. Komaki and F. Fujimoto, Phys. Lett. 49A, 445 (1974).

²²A. Tamura and T. Kawamura, Phys. Status Solidi 73B, 391 (1976).

²³S. A. Vorob'ev, S. V. Plotnikov, I. A. Tsekhanovskii, and V. P. Koshcheev, Izv. Akad. Nauk SSSR Ser. Fiz. 9, 164 (1976).

²⁴U. Schiebel and E. Worm, Phys. Lett. 58A, 252 (1976).

²⁵V. V. Kaplin, D. E. Popov, and S. A. Vorob'ev, Phys. Status Solidi 76B, 309 (1976).

²⁶Yu. M. Kagan and Yu. V. Kononets, Zh. Eksp. Teor. Fiz. 58, 226 (1970) [Sov. Phys. JETP 21, 124 (1970)].

²⁷A. A. Vorob'ev, V. V. Kaplin, and S. A. Vorob'ev, Nucl. Instrum. Methods 127, 265 (1975).

²⁸M. A. Kumakhov, Dokl. Akad. Nauk SSSR 230, 1077 (1976) [Sov. Phys. Dokl. 21, 581 (1976)].

²⁹V. A. Belyakov, Pis'ma Zh. Eksp. Teor. Fiz. 13, 254 (1971) [JETP Lett. 13, 179 (1971)].

Translated by J. G. Adashko